Torres-Carrasco, M.; Puertas, F. (2015). Waste glass in the geopolymer preparation. Mechanical and microstructural characterisation, *Journal of Cleaner Production*, v. 90, pp.: 397-408.

DOI: https://doi.org/10.1016/j.jclepro.2014.11.074

Waste glass in the geopolymer preparation. Mechanical and microstructural characterisation

M. Torres-Carrasco[1], F. Puertas[1]*

[1]Eduardo Torroja Institute for Construction Science (IETcc-CSIC),
C/ Serrano Galvache 4, 28033 Madrid, Spain
*Corresponding author: e-mail address: Prof. Francisca Puertas (puertasf@ietcc.csic.es)

ABSTRACT

Alkali activated materials have a variety of niche applications (other than as a large-scale civil infrastructure material) in which alkali-activated binders and concretes have shown potential for commercial-scale development. The majority of these applications have not yet seen large-scale alkali activated materials utilisation, moreover, there have been at least pilot-scale or demonstration projects in different areas and each provides scope for future development and potentially profitable advances in science and technology. This paper explores the feasibility of generating geopolymers from fly ash using waste glass as an alkaline activator (waterglass family). The mechanical properties of the cementitious geopolymers obtained by alkali-activating fly ash with three solutions: sodium hydroxide 8M, sodium hydroxide 10M + 15 % waterglass and sodium hydroxide 10M + 15 g of waste glass were determined, along with their microstructural characteristics using Fourier Transform Infrared Spectroscopy, X-Ray Diffraction, Mercury Intrusion Porosimetry, Mass Nuclear Magnetic Resonance, Scanning Electron Microscopy and Back Scattering Electron Microscopy. The main reaction product in all the systems studied was the alkaline aluminosilicate hydrate gel to which geopolymers owe their mechanical properties. The gel formed when the system contained an extra source of silicon was shown to prompt compositional differences, while the degree of reaction, microstructure and Si/Al and Na/Al ratios were very similar in the former two systems. Waste glass proved to be an effective alkaline activator in geopolymer preparation.

Keywords: geopolymers, waste glass, mechanical strength, characterisation, alternative alkaline activators

1. Introduction

Portland cement-based products, primarily concretes, are the world's most commonly used building materials. The world Ordinary Portland Cement (OPC) industry, however, is facing a number of highly sensitive issues with a social impact. The economic-energy problems implicit in the use of ever more costly and scarce fossil fuels and heavy thermal and electrical power

consumption are aggravated by ecological questions, for the manufacture of 1 tonne of cement calls for 1.7 tonnes of prime materials and involves the emission of 0.8 tonnes of CO_2 into the atmosphere (Hendriks et al., 2000; U.S. Environmental, 2004; Huntzinger and Eatmon, 2009). Cement manufacture is estimated to account for around 6-7 % of global CO_2 emissions (Scrivener and Kirkpatrick, 2007). At the 2014 World Economic Forum held at Davos, the European Commission defined the EU's climate and energy objectives for 2030 with a proposal that would entail a 40-% emissions abatement from 1990 levels over the next 16 years. In addition, the Commission announced that the renewable energy generation target for the EU as a whole would be 27 %. In Spain, a party to that agreement, emissions have risen substantially in recent years. The need to lower its emissions has prompted the construction industry to seek valid alternatives in the form of new binders such as the so-called alkali-activated materials (AAMs), prepared by alkali-activating industrial waste and by-products, including slag, fly ash and silica fume (Puertas, 1995; Palomo et al., 1999). The manufacture of these new cements and concretes is characterised by lower energy demands than OPC production, as well as lower polluting gas emissions and the absence of durability-related technical problems. These binders are also known as alkaline cements.

Alkaline cements, initially proposed by Glukhovsky (Glukhovsky, 1965; Glukhovsky, 1989), consist essentially of two components: a powdery aluminosilicate-based material (such as blast furnace slag, fly ash or metakaolin) and an alkaline activator. The reactions taking place during alkaline activation can be regarded as a series of complex transformations in the starting solid which ultimately yield a condensed structure with cementitious properties. These end products have been variously baptized as "geopolymers" (Davidovits, 1991), "vitreous aluminosilicates synthesised at low temperatures" (Rahieret al., 1996), "alkali-activated cements" (Palomo and López de la Fuente, 2003), "geocements" (Krivenko, 1994), and inorganic polymers (Van Wazer, 1970).This study focused on the alkaline activation of type F fly ash, a by-product of coal-fuelled steam power plants that generates the type of binders to which the term geopolymer is best suited.

An additional incentive for using fly ash is that as an energy industry by-product, if it goes unused it has to be deposited in controlled sanitary landfills. One tonne of ash is estimated to occupy a volume similar to 928 kg of municipal solid waste (Ukqaa, 2014), thereby shortening the service life of landfills considerably. The European Coal Combustion Products Association (ECOBA) estimated that in 2010 the EU-27 generated 105 million tonnes of coal combustion products (CCPs). Fly ash, with 86 million tonnes yearly, constituted 81 % of the total (ECOBA, 2014).

The alkaline solutions able to interact with aluminosilicates to generate these new binders include: alkaline metal or alkaline-earth hydroxides (ROH, $R(OH)_2$), weak acid salts (R_2CO_3, R_2S, RF), strong acid salts (Na_2SO_4, $CaSO_4 \cdot 2H_2O$) and $R_2O(n)SiO_2$-type siliceous salts, where R is an alkaline ion such as N, K or Li. From the standpoint of end product strength and other properties, the most effective of these activators are NaOH, and sodium silicate hydrate (waterglass) (Provis, 2009; Palacios and Puertas, 2007). And of these, the solutions that induce the best mechanical behaviour in alkali-activated materials are waterglass-based (Fernández-Jiménez et al., 1999; Fernández-Jiménez and Palomo, 2005a; Kovalchuk et al., 2007). In the industrial production of sodium silicate or waterglass, however, temperatures of around 1 300 °C must be reached to fire the carbonate and silica salts that are subsequently dissolved in water in suitable proportions (Larosa-Thomson et al., 1997; Brykov and Korneev, 2008). Nonetheless, materials such as silica fume, pozzolans or rice husk ash can also be used as supplementary sources of silica in these alkali-activated systems (Mejía et al., 2013). Their use both valorises industrial waste or by-products and minimises the adverse effects (energy consumption and CO_2 emissions) of industrial waterglass production (Yang et al., 2013; Yang et al., 2014).

Pastes, mortars and concretes made with alkali-activated fly ash develop very high early age (1-day) mechanical strength, which continues to grow over time, albeit more slowly. They also exhibit beneficial physical-chemical properties such as scant drying shrinkage and excellent matrix-steel bonding (pull-out test) (Hardjito et al., 2002; Fernández-Jiménez et al., 2006a). Another important feature of these materials is their durability against chemical attack in even the most aggressive environments: sea water, sulfate attack, acid media and high temperatures (Fernández-Jiménez et al, 2007).

The present study aimed to evaluate the feasibility of using urban and industrial waste, and more specifically glass, as a source of silica to replace sodium silicate (waterglass) in the alkaline activation of fly ash. Urban waste glass is an amorphous material with a chemical composition consisting essentially of SiO_2 (65-75 %), CaO (6-12 %), Na_2O (12-15 %), Al_2O_3 (0.5-5%) and Fe_2O_3 (0.1-3 %) (Torres-Carrasco et al., 2014; Torres-Carrasco et al., 2012; Puertas et al., 2012a).

One of the most prominent properties of glass, in addition to its transparency, is its high resistance to chemical attack. That notwithstanding, some interaction always takes place between glass and chemical substances. Glass is attacked by both acid and alkaline solutions, although the mechanisms and degree of corrosion differ (Fernández Navarro, 2003). These

materials are highly soluble in alkaline solutions (pH values of over 10.7) (El-Shamy et al., 1972; El-Shamy and Panteno, 1977; Paul, 1977), which dissolve amorphous silica to form soluble silicate. Raising the temperature favours glass solubility (Paul, 1977; Goto, 1955).

Prior studies determined the solubility of different types of urban and industrial waste glass in highly alkaline media (Torres-Carrasco et al., 2014; Torres-Carrasco et al., 2012; Puertas et al., 2012a). This waste has been found to dissolve most effectively (highest amounts of dissolved SiO_2 and Al_2O_3) in a 50/50 solution of $NaOH/Na_2CO_3$ heated at 80 °C for 6 h (Torres-Carrasco et al., 2014; Puertas et al., 2012b; Puertas and Torres-Carrasco, 2014). The question is whether these solutions prepared with waste glass can replace traditional waterglass in the manufacture of geopolymers and alkaline cements, as they have been shown to be able to do in alkali-activated slag (AAS) systems (Puertas and Torres-Carrasco, 2014).

Actually, in addition to the civil infrastructure, there are a number of areas in which alkali-activation chemistry has been shown to provide the potential for utilisation in niche applications in various areas of civil and materials engineering. It is certainly possible to tailor alkali-activated materials for applications in lightweight materials production, as well cement for underground utilisation, for high-temperature applications, as a stabilisation/solidification matrix for hazardous or radioactive wastes, etc (Bernal et al., 2014; Mendes et al., 2008; Medes et al., 2009).

Consequently, the primary objective of the present research was to explore the feasibility of using urban and industrial waste glass as a potential alkaline activator in the preparation of geopolymers with fly ash.

2. Experimental program

A type F fly ash (ASTM C618-03) furnished by the Puentenuevo steam plant in the Spanish province of Cordoba and urban glass waste provided by the city of Madrid's waste management service were used as starting materials. According to the chemical compositions given in **Table 1,** Si, Al and Fe were the most abundant oxides present in the fly ash, followed by Ca, Mg and alkaline (Na and K) oxides. The SiO_2/Al_2O_3 ratio in the fly ash was ≈2. In fly ash alkaline activation, the percentage of reactive silica is an important factor, for this silica reacts with the alumina and alkalis to generate cementitious systems (Fernández-Jiménez and Palomo, 2003a). This fly ash had a reactive silica content of 45.05 % (**Table 2**).

Table 1. Chemical composition of fly ash and waste glass (wt.%)

Table 2. Reactive SiO_2 and Al_2O_3 content in fly ash

Three alkaline activators were used NaOH 8M, NaOH 10M + 15 % waterglass and a solution of NaOH10M mixed with different proportions of glass (10, 15 and 25 g per 100 mL of solution). The products used to prepare the activating solutions were laboratory reagents: NaOH in the form of 98 % pure pellets (PANREAC) and sodium silicate (MERCK) containing 27 % SiO_2, 8 % Na_2O and 65 % H_2O (by weight). The aforementioned amounts of glass (particle size of under 45 μm) were mixed with the solution of NaOH 10M and magnetically stirred at 80 ± 2 °C for 6 hours. The solution was subsequently filtered and the liquid used as the activator. The procedure is described in (Torres-Carrasco et al., 2014). The ion concentration in the filtered solutions were analysed by ICP-AES on a VARIAN 725-ES inductively coupled plasma atomic emission spectrometer (see **Table 3**).

Table 3. SiO_2, Al_2O_3, CaO and MgO content (g/100 ml) in solutions prepared by dissolving waste glass in 100 mL of 10-M NaOH

2.1 Paste preparation and trials conducted

Paste specimens measuring 1x1x6 cm were prepared for all the systems with a constant liquid/solid ratio of 0.3 to ensure that plasticity was as recommended in European standard EN 196-3. The activation conditions used to prepare the geopolymers are listed in **Table 4**. The pastes were cured pursuant to the "curing in covered moulds (CCM)" technique (Kovalchuk et al., 2007). This procedure, used in prior research, ensures that humidity is held constant to prevent quick setting (Krivenko et al., 2002a; Krivenko et al., 2002b; Kovalchuk, 2002) and carbonation (Criado et al., 2005) while the material sets and hardens. The trial consisted of placing the moulds with the fresh paste in sealed individual plastic bags to prevent water evaporation during initial oven curing for 20 hours at 85 °C. The pastes were subsequently cured in a chamber at 99 % relative humidity and 20 ± 2 °C until the test date (1, 2, 7 or 28 days).

The prismatic specimens were tested for compressive strength. After the mechanical tests, the pastes were treated with acetone/ethanol to detain hydration/activation for subsequent analysis via Hg intrusion porosimetry, X-ray diffraction (XRD), Fourier transform infrared (FTIR) spectroscopy, ^{29}Si and ^{27}Al nuclear magnetic resonance (^{29}Si and ^{27}Al NMR) and backscattered electron microscopy (BSEM/EDX).

Table 4. Geopolymer preparation: activation conditions

Bending and compressive strength tests were conducted to failure on an Ibertest Autotest 200/10 hydraulic press at a rate of 2 400 N/s ± 200 N/s as specified in European standard EN 196-1. Total porosity and pore size distribution were found with Hg intrusion porosimetry on a Micromeretics Autopore IV 9500 analyser able to exert pressure of up to 32 000 Psi (equivalent to a pore size as small as 0.0067 µm). The XRD patterns for the samples were recorded on a Bruker AXS D8 Advance diffractometer fitted with a Lynxeye super speed XR detector and a 2.2-kW Cu anode. No monochromator was used. The scanning range, from (2θ) 5 to 50°, was covered in a 24-minute period. The instrument was set at 40 kW and 30 mA and the sample was not rotated during scanning. The FTIR spectra were obtained by analysing compressed KBr pellets containing 1.0 mg of sample in 300 mg of KBr on an ATIMATTSON Genesis Series FTIR-TM spectrometer. The solid state nuclear magnetic resonance (^{29}Si and ^{27}Al MAS NMR) spectra were obtained from 64 scans run on a Bruker MSL 400 spectrometer operating at a range of 4 000 to 400 cm^{-1} and 79.49 and 104.26 MHz, respectively. All the samples were placed in a 4-mm zirconium MAS rotor and spun at 10 000 Hz. For the ^{27}Al spectra, the relaxation time applied was 5 seconds and 360 acquisitions were obtained per scan. For the ^{29}Si spectra, the values were 10 seconds and 1 200 acquisitions. After the spectra were recorded, the curves were deconvoluted with dmfit software, which fits the theoretical to the experimental curves. Seven-day samples were embedded in an epoxy resin and cut, polished and carbon-coated for examination under a JOEL JSM 5400 scanning electron microscope equipped with a solid-state backscattered detector and LINK-ISIS energy dispersive (EDX).

After thermal curing, the alkali activated fly ash was attacked with 1:20 HCl to determine the degree of reaction (α) at 7-day hydration. The experimental procedure followed in the acid attack consisted of adding 1 g of activated fly ash to a beaker containing 250 ml of (1:20) HCl.

The mixture was stirred with a plastic rotor for three hours, after which it was filtered and washed with de-ionized water to a neutral pH. The insoluble residue was first dried at 100 °C and then calcined at 1 000 °C; the degree of reaction, α, was found by determining weight loss (**Figure 1**) (Fernández-Jiménez et al., 2006b).

Figure 1. Experimental method for quantifying the degree of reaction of the alkali cements prepared and the SiO_2/Al_2O_3 ratios of the reaction products generated during alkali activation

3. Results and discussion

From the chemical standpoint, the most important factor in geopolymer formation is the silica and reactive alumina content in the starting aluminosilicate, because silicon is the main component of the structural skeleton of the reaction products formed during alkaline activation of the material. Together with dissolved aluminium, in high alkalinity media it forms poly-hydroxysilicoaluminate-type complexes (Fernández-Jiménez and Palomo, 2003a; Fernández-Jiménez et al., 2006c; Palomo et al., 2004a; Weng et al., 2005). The end product is a N-A-S-H-type alkaline aluminosilicate hydrate, also known in the literature as a geopolymer. Both the Al and the Si are tetrahedrally coordinated in the reaction product, while the alkalis (Na or K) positioned in the voids in the three-dimensional structure offset the electrical charge generated when Al^{3+} replaces Si^{4+} ions. Schematically, the process may be described as follows (1):

$$n(Si_2O_5,Al_2O_2) + nH_2O + NaOH \rightarrow Na^+ + n(OH)_3\text{-}Si\text{-}O\text{-}Al^-(OH)_2\text{-}O\text{-}Si\text{-}(OH)_3 \rightarrow \quad (1)$$

$$\rightarrow Na^+ (\text{-}Si\text{-}O\text{-}Al\text{-}O\text{-}Si\text{-}O\text{-}) + nH_2O$$

Aluminosilicate gel or zeolite precursor

This aluminosilicate gel, which can be regarded as a zeolite precursor (Alonso and Palomo, 2001), is the constituent that affords these systems their mechanical properties (Palomo et al., 1999; Fernández-Jiménez and Palomo, 2003b). Consequently, a high reactive silica content

induces the formation of a high aluminosilicate (N-A-S-H) gel content and with it high mechanical strength.

3.1 Mechanical performance and Hg porosimetry

The compressive strength developed by the oven-cured, 1x1x 6 cm activated fly ash specimens are plotted in **Figure 2**. Mechanical strength was observed to rise when a solution of NaOH 10M was used instead of a NaOH 8M solution, denoting the high concentration of alkalis as well as the high pH value required by these systems (see data in **Table 4**). Moreover, when SiO_2 (present in the commercial waterglass solution) was added to the activating solution, strength rose to 28-day values of around 37 MPa and 1-day values of 30 MPa. When the source of the SiO_2 in the solution was waste glass, even higher strength values were observed. The best results were obtained with 15 g in 100 mL of NaOH 10M (**Figure 2b**), which yielded strength greater than the 37 MPa observed with commercial waterglass. An excess of waste glass (25 grams), however, lowered strength to values below the findings for NaOH 8M. This can be explained in terms of the solution pH (see **Table 4**), which declined considerably as the content of Si from the waste glass in the medium rose, as well as in terms of the SiO_2/Na_2O ratio. According to the values in **Table 4**, the SiO_2/Na_2O ratio for the waterglass solution was 0.19. As the waste glass content in the medium grew, the dissolved silicon also grew (see **Table 3**), and with it the SiO_2/Na_2O ratio, up to values of 0.16 in the solution with 25 g of glass. In contrast, the solution containing 15 g of glass, which delivered the best results, had a SiO_2/Na_2O ratio of 0.11 and a pH closer to the pH of the waterglass solution.

The variation in the SiO_2/Na_2O ratio in these solutions may entail changes in the degree of polymerisation of the dissolved chemical species. McCormick (McCormick et al., 1987a; McCormick et al., 1987b), studying the effect of the silicate ratio, $R = [SiO_2]/[Na_2O]$ on silicon atom connectivity, concluded that the higher the ratio, the greater the connectivity among silicon atoms. Analogously, therefore, when the SiO_2/Na_2O ratio rises in these systems, the degree of polymerisation also rises. Further to these studies, when 15 g of waste glass were added to 100 mL of NaOH 10M, the dissolved silica was essentially monomeric (Torres-Carrasco et al., 2014; Puertas and Torres-Carrasco, 2014), but as the glass content grew, the solution may have become saturated, hindering the full solubilisation of the glass and inducing a higher degree of polymerisation.

Figure 2. a) Compressive strength of fly ash pastes activated with different alkaline solutions; b) compressive strength of specimens prepared with NaOH 8M, NaOH 10M + 15 % WG and NaOH 10M + 10, 15 or 25 g of waste glass

The compressive strength values observed in the pastes could be explained on the grounds of the mercury intrusion porosimetry findings. As **Figure 3** shows, total porosity did not vary significantly over time, because the geopolymerisation reaction took place and was accelerated by the heat (85 °C) applied during the first 20 hours. The largest share of reaction products were generated in that first period and redistributed over time to form more cohesive structures. In systems with 100 % fly ash as the binder, alkaline activation of the ash particles and the formation of the reaction products hold material porosity more or less constant throughout the hardening process (Zeng et al., 2010). In this study, the pastes with the lowest total porosity were the ones activated with the NaOH 10M + WG solution. Total early age porosity was greatest in NaOH 8M-activated fly ash paste, where it ranged from 23 to 26 %. In the pastes prepared with Si-containing activators, total porosity was slightly lower: 22-25 % in both NaOH 10M + WG and NaOH 10M + glass. Analysis of the pore size distribution revealed that small pores (0.1-1 μm) accounted for a higher fraction in all the pastes. These total porosity and pore size distribution findings are consistent with the compressive strengths described above (**Figure 3**).

Figure 3. Pore size distribution in NaOH 8M, NaOH 10M + WG and NaOH 10M + glass AAFA

3.2 Characterisation of reaction products

A mineralogical and microstructural analysis was conducted on the geopolymer pastes to explain and understand the mechanical performance described earlier. The study was conducted on the 7-day alkali-activated ash pastes prepared with the experimental solutions: NaOH 8M, NaOH 10M + 15 % WG and NaOH 10M + 15 g waste glass. The third was selected as it was the solution with waste glass that yielded the highest mechanical strength.

3.2.1 XRD and FTIR

Reaction products are characterised mineralogically with XRD to identify the crystalline components in the system. **Figure 4a** reproduces the X-ray diffractograms for the 7-day activated pastes, as well as the diffractogram for the original fly ash. In all cases, the diffraction pattern changed appreciably after the fly ash was activated. One change was the shift in the

position of the halo attributed to the vitreous phase in the initial ash to slightly higher 2θ angles, an indication of the presence of an alkaline aluminosilicate (N-A-S-H) gel, the main reaction product. The minority crystalline phases (quartz, mullite and magnetite) detected in the initial material remained apparently unaltered.

Zeolite-like crystalline phases appeared on the post-activation spectra. The type of zeolite that crystallised depended on the activating solution used. Zeolite species such as sodalite hydrate ($Na_4Al_3Si_3O_{12}OH$, JCPDS 11-0401) with a Si/Al ratio of 1 (Breck, 1973) and chabazite-Na ($NaAlSi_2O_6{\cdot}3H_2O$, JCPDS 19-1178) with a Si/Al ratio of 2 (Breck, 1973) were detected on the diffractogram for the 7-day geopolymer formed from fly ash activated with the NaOH 8M solution (**AAFA N8**). Zeolite species such as sodalite hydrate and chabazite-Na were also observed when waterglass (**AAFA WG**) was the activator. In this case, the chabazite-Na-type zeolite content was found to rise because the larger amount of silica in the medium (NaOH 10M + 15 % WG) favoured its early crystallisation. When the source of the silica was dissolved waste glass (15 g per 100 mL of NaOH 10M; **AAFA N10-15**), the resulting diffractogram resembled the diffractogram for the paste prepared with WG very closely: i.e., considerable amounts of chabazite-Na were observed to form. Nonetheless, according to other studies (Criado et al., 2007), a considerable rise in the silica content in the medium retards the formation of zeolite species, inducing a decline in mechanical strength due to the absence of N-A-S-H gel.

Figure 4b shows the FTIR spectra for the 7-day geopolymers obtained after activating the fly ash with the three solutions. These materials contained both unreacted particles and reaction products (sodium aluminosilicate gel, the majority product, and minority crystalline zeolites). All these products consisted primarily of SiO_4 and AlO_4tetrahedra.

Figure 4. a) XRD for fly ash and alkali-activated fly ash pastes; b) FTIR spectra for fly ash and alkali-activated fly ash pastes.

An analysis of the spectra showed that the most characteristic bands were: a main band at around 1 000 cm^{-3} associated with the asymmetric vibrations generated by T-O-T bonds (where T is Si or Al). In all the systems, regardless of the type of activator used, this band, located at around 1 060 cm^{-1} in the original fly ash, narrowed and shifted to lower frequencies after the fly ash was activated: to around 1 010 cm^{-1} (**AAFA N8**), 1 003 cm^{-1} (**AAFA WG**) and 1 004 cm^{-1} (**AAFA N10-15**). These shifts indicate that the glass component in the fly ash reacted

with the alkaline activator to form reaction products, primarily N-A-S-H, an aluminosilicate gel (Fernández-Jiménez and Palomo, 2005b). The exact position of this band depended on the Si/Al ratio of the product formed. The shift was to lower frequencies due to the rise in the tetrahedral aluminium content (Fernández-Jiménez and Palomo, 2005b). With the replacement of Si^{4+} by Al^{3+}, the T-O-T angle became more acute, shifting the signal to lower frequencies due to the weaker bond and to the fact that the Al-O bond is longer than the Si-O bond. The shift in these bands was observed to be more intense in the pastes activated with NaOH 10M + 15 % waterglass and NaOH 10M + 15 g of waste glass than in the pastes activated with NaOH 8M. That means that the Si content was higher in the reaction products in the former two than in the latter (Fernández-Jiménez and Palomo, 2005b; Mozgawa et al., 1999). The rest of the bands characteristic of N-A-S-H gel between 800 and 500 cm^{-1}, which were also present, were associated with the vibrations generated by the tetrahedra formed. A series of bands attributed to the presence of zeolites (detected with XRD) also appeared.

3.2.2 Nuclear magnetic resonance (MAS NMR ^{29}Si and ^{27}Al)

Figure 5 shows the ^{29}Si MAS NMR spectrum for unreacted fly ash. It is characterised by a very wide and ill-defined profile, indicative of the uneven distribution of the silicon atoms in this type of material. Spectrum deconvolution revealed the presence of nine main signals (**Table 5**), (≈-78.59, -83.77, -94.82, -99.72, -104.38 and -108.90 ppm, with an error of ± 1 ppm), associated primarily with the glass phase in the material (Fernández-Jiménez and Palomo, 2003a; Fernández-Jiménez et al., 2006b). The signal at -89.21 ppm, in turn, was assigned to the Q^3 (3Al) Si units in the mullite present in fly ash (Gomes and François, 2000). Lastly, the signals at values higher than -113.89 and -118.67 ppm were attributed essentially to the presence of different forms of crystalline silica (Q^4 (0Al) signals) (Engelhardt and Michel, 1987).

Table 5.Deconvolution of the ^{29}Si MAS NMR spectrum for fly ash

The ^{29}Si NMR spectra for the geopolymers generated after the interaction between the fly ash and the various alkaline solutions are shown in **Figure 6**. The changes detected between these spectra and the spectrum for the starting fly ash can be attributed to chemical changes taking place during alkaline activation. The experimental signals were deconvoluted using references extracted from prior studies (Fernández-Jiménez et al., 2006c; Palomo et al, 2004a; Engelhardt

and Michel, 1987; Klinowski, 1984). The present analysis assumed a constant band width for all components.

Figure 5. ^{29}Si NMR spectra for the starting fly ash

The ^{29}Si MNR spectra obtained for the 7-day pastes activated with the various solutions used in this study contained signals at around -84, -88, -93, -99, -104 and -108 ppm (with an error of ± 1 ppm). The area of the signal at around -84 ppm, attributed to the hydroxysodalite-type $Q^4(4Al)$ units detected by XRD (see **Figure 4a**), remained practically unaltered in all the systems. The signals at around -88, -93, -99, -104 and -108 ppm were associated with silicon tetrahedra surrounded, respectively, by Al_4, $SiAl_3$, Si_2Al_2, Si_3Al_1 y Si_4, all with a chabazite-Na-like structure. The signal at around -108 ppm was associated with $Q^4(0Al)$ units such as highly polymerised quartz-like (-108/-109 ppm) or cristobalite-like (-113/-114 ppm) silica (Engelhardt and Michel, 1987). The ^{29}Si NMR spectra for the pastes obtained by activating fly ash with NaOH 8M and NaOH 10M + 15 % waterglass solutions were similar, although the most intense signal (≈-98, -99 ppm) was much more clearly defined in the latter, so that the addition of a small amount of soluble monomeric silica therefore can be said to induce different reaction products (Torres-Carrasco et al., 2014; Puertas and Torres-Carrasco, 2014; Criado et al., 2008). Much the same was observed when the solution used was NaOH 10M + 15 g of glass waste, in which the procedure for dissolving the silica (6 hours at 80 ± 2 °C) yielded monomers (Torres-Carrasco et al., 2014; Puertas and Torres-Carrasco, 2014) with a reactivity similar to the reactivity observed in the NaOH 10M + 15 % waterglass solution. That would explain the compressive strength values found (see **Figure 2**).

Table 6. ^{29}Si NMR signals for 7-day alkali activated fly ash

A comparison of the ^{29}Si MAS NMR spectra for all the pastes obtained by activating the fly ash with different solutions revealed that the end, and consequently the most thermodynamically stable, product formed was similar in all cases. The formation kinetics of this compound varied, however, depending on the nature of the activator. All the spectra were typical of the formation of an aluminosilicate gel (N-A-S-H gel) with high silicon content. These spectra for 7-day pastes exhibited five main signals, associated with silicon surrounded by zero, one, two, three or four aluminium tetrahedra in the aluminosilicate gel. Their signals appeared at around -110, -104, -98, -93 and -88 ppm respectively (with an error of ± 1 ppm). Nonetheless, in the

AAFA WG and AAFA N10-15 systems, the presence of soluble silica in the medium sourced from the activator itself would be expected to affect the initial dissolution of the ash and the nature of the early age species formed: from the outset, the Al released would react with the silicon ions in the solution to form compounds whose Si/Al ratios were greater than 1. The Si/Al ratios were found with the Engelhardt (Engelhardt and Michel, 1987) equation (2), in accordance with Lowenstein's rule. The Engelhard equation is defined as:

$$(Si/Al)_{NMR} = \frac{\sum_n In(SinAl)}{0.25\sum_n nIn(SinAl)} \qquad n = 0, 1, 2, 3 \text{ y } 4 \qquad (2)$$

where $I_n(Si_nAl)$ is the intensity of the component associated with a silicon surrounded by nAl and (4-n)Si. As **Table 6** shows, the Si/Al ratios obtained with the Engelhard equation were similar for the AAFA WG and AAFA N10-15 systems. That confirmed that the nature of the activating solution played an important and analogous role in the two systems as a source of soluble silica in the medium, inasmuch as the ratio found for the NaOH 8M solution was slightly lower. This was subsequently verified by the degree of reaction and the percentage of dissolved silica and alumina found after the 1:20 HCl attack (see **Table 7**) and BSEM/EDX exploration (see **Table 8**). Moreover, gel formation kinetics were conditioned by the amount and type of polymeric species present in the solution while, as noted earlier, the existence of monomeric species in both systems (AAFA WG and AAFA N10-15) led to very similar compositions in the two gels. Signal of this lies in the much more intense shift in the T-O-T bands on the FTIR spectra.

Figure 6.^{29}Si MAS NMR spectra of alkali activated fly ash pastes: AAFA N8, AAFA WG and AAFA N10-15.

The ^{27}Al MAS NMR spectrum for the original fly ash contained two signals, one centred at + 50.4 ppm, associated with tetrahedral aluminium units (Al_T) and another more poorly defined at + 4.81 ppm attributed to octahedral aluminium units (Al_O). The octahedral signal was attributed to the octahedral aluminium in the mullite present in the original fly ash (Engelhardt and Michel, 1987).

After alkaline activation, the signal for the tetrahedral aluminium, initially positioned at around + 50 ppm, shifted to + 58-59 ppm in all systems, indicating that the aluminium always retained

its tetrahedral coordination. This signal was attributed to an aluminium atom surrounded by four silicon tetrahedra, a configuration characteristic of zeolite precursor (AlQ^4 (4Si) environments (Fernández-Jiménez et al., 2006c).

3.2.3 Determination of the degree of reaction (1:20 HCl)

The degree of reaction and SiO_2/Al_2O_3 ratio of the reaction products generated in each cementitious system were quantified as described in **Figure 1**, with a view to exploring the above findings in greater depth. The degree of reaction and the SiO_2/Al_2O_3 ratio of the alkaline activation products were quantified to determine whether the end properties of the geopolymers obtained through activation can be forecast from the percentage of reactive phase and the reactive SiO_2/Al_2O_3 ratio in the starting fly ash.

Table 7 gives the degree of reaction for each alkali-activated fly ash system at 7-day hydration. The highest value (34.1 %) was obtained with the solution containing NaOH 10M + 15 g of waste glass. That is consistent with and explains the slightly higher strength values observed (see **Figure 2**) for 7-day AAFA N10-15 than for AAFA WG (whose degree of reaction was 31.6 %). Moreover, a rise in the SiO_2/Al_2O_3 ratio in the reaction products would also explain the compressive strength values. Nonetheless, as the SiO_2/Na_2O ratio was slightly higher in the waterglass than in the NaOH 10M + 15 g of waste glass solution (see **Table 4**), the SiO_2/Na_2O ratio was higher in the AAFA WG system due to the higher content of dissolved monomeric silica in the commercial solution.

Table 7. Degrees of reaction, percentage of dissolved silica and alumina after a selective 1:20 HCl attack on alkali-activated systems. SiO_2/Al_2O_3 ratio of the reaction products

3.2.4 Compositional study of the gel with backscattered electron microscopy (BSEM/EDX)

Backscattered electron microscopy (BSEM) was used to determine the Si/Al and Na/Al ratios in the sodium aluminosilicate (N-A-S-H) gels. The findings are listed in **Table 8**. Twenty acquisitions were performed for the elemental analysis of each sample.

Table 8. BSEM/EDX-determined chemical composition of 7-day sodium aluminosilicate gel obtained by activating fly ash with three solutions

The elemental composition of aluminosilicate gel consisted primarily of silicon, aluminium and sodium, with smaller percentages of calcium, magnesium, potassium and iron. This technique aims to study the main elemental constituents in the gel and observe their variations with the amount of soluble silica in the medium.

Figure 7. BSEM/EDX images of a) AAFA N8, b) AAFA WG, c) AAFA N10-15 pastes

All the evidence appeared to indicate that raising the silica content in the activating solution translated into a higher Si/Al ratio in the N-A-S-H gel (**Table 8, Figure 7**). The Si/Al ratio in the gel formed in the NaOH 8M system was slightly lower than the ratio found when the activator used was NaOH 10M with 15 % waterglass or the solution containing waste glass. When the activator contained Si, the Al and Na content in the medium declined; moreover, the gels in the NaOH 10M + 15 % WG and NaOH 10M + 15 g waste glass solutions exhibited identical Si/Al ratios. These results corroborated the percentages of dissolved silica and alumina (see **Table 7**) found by the HCl attack, according to which the Si/Al ratios were very similar in these two systems and higher than in the AAFA N8 systems. Here also, the similarity in the behaviour of waste glass and waterglass is an indication that the former shows promise as a possible substitution for commercial sodium silicate.

The SEM microstructural study provided insight into geopolymer formation and how it was affected by the nature of the activating solution. In the earliest stages of the reaction, the alkaline solution dissolved part of the outer shell of the fly ash particles, exposing the smaller particles (located inside the larger ash) to alkaline attack. In that stage the reaction mechanism involved was dissolution. An amorphous aluminosilicate (N-A-S-H) gel, the main reaction product, was observed alongside unreacted spheres.

When the alkaline activator was the NaOH 8M solution (AAFA N8), the microscopic image exhibited a considerable number of pores and a series of hollow spheres (**Figure 7a**). The reaction product was detached from the individual spheres, forming an unevenly distributed solid mass in contact with the unreacted particles. That some ash spheres were partially covered by reaction product suggested that over time, reaction product may precipitate onto the unreacted particles, forming a film that would hamper the subsequent activation of the latter (Palomo et al., 2004b).

In addition to the sodium aluminosilicate gel, the partially reacted ash particles or the pores left after they reacted fully were observed to contain crystalline deposits. These crystals would be the zeolites detected by XRD. **Figure 8** shows the minority phases present, such as a chabazite-Na-like zeolite, which consists of a series of macles that congregate to form what looks like a ball of wool.

Figure 8. Detail of crystalline phases (chabazite-Na-like zeolite) formed in fly ash pastes activated with NaOH8M(AAFA N8)

The pastes activated with the waterglass solution (AAFA WG) (**Figure 7b**) also exhibited crystallised chabazite-Na-like zeolites in the voids inside the partially reacted ash particles or the pores left by these particles after reacting completely (**Figure 9**). These zeolites (minority phases), visible in the micrograph, were apparently identical to the ones formed in system AAFA N8, although with a higher silicon content and more perfect crystallisation than in that system, as corroborated by the XRD findings.

Figure 9. Detail of crystalline phases (chabazite-Na-like zeolite) formed in fly ash pastes activated with NaOH 10M+ 15 % WG (AAFA WG)

Lastly, when the ash was activated with the NaOH 10M + 15 g waste glass (AAFA N10-15) solution; its morphology resembled the morphology observed in the gel activated with the NaOH 8M solution, with chabazite-Na as the main zeolite (**Figure 10**). Nonetheless, the elemental analysis of the sodium aluminosilicate gel revealed that its Si/Al ratio was very similar to the ratio found for the waterglass solution (**Table 8, Figure 7**). In other words, the soluble silica from the waste glass formed part of the gel, inducing a rise in zeolite formation and with it higher strength values.

Figure 10. Detail of crystalline phases (chabazite-Na-like zeolite) formed in fly ash pastes activated with NaOH 10M + waste glass (AAFA N10-15)

4. Conclusions

Waste glass has been proven to be a viable substitute for the commercial sodium silicate hydrates (waterglass) commonly used to prepare geopolymers by activating aluminosilicate materials such as fly ash.

The main reaction product in the alkaline activation of fly ash is an amorphous polymer, an aluminosilicate hydrate (N-A-S-H gel) whose chemical composition and microstructure vary depending on the nature of the activator used. That factor plays an instrumental role in the kinetics, structure and composition of the gel initially formed, in which the dissolved silicate from the NaOH 10M + 15 % waterglass and NaOH 10M + 15 g waste glass solutions had a substantial impact on the composition of the reaction products.

The microstructural analyses performed in this study contribute to the understanding of the gels forming in these systems. FTIR showed that as the fly ash was activated, the band characteristic of asymmetric T-O bond stretching shifted to lower frequencies, particularly in the systems with an additional amount of silicon in the medium, present in the commercial waterglass solution (AAFA WG) or in the solution containing waste glass (AAFA N10-15).

Further to the ^{29}Si NMR findings, both the intensity of the signals for the N-A-S-H gel and its Si/Al ratio, determined with the Engelhard equation, were similar in the AAFA WG and AAFA N10-15 systems (ratios of 2.04 and 2.01, respectively). The Si/Al ratio found with ^{29}Si NMR was confirmed by the results of a selective 1:20 HCl attack on the gels to determine the percentage of dissolved silica and alumina. The degree of reaction in these systems was, moreover, higher than in system AAFA N8, providing a further explanation of the better mechanical performance of the pastes formed in media with additional silicon.

Lastly, the BSEM/EDX and SEM microscopic studies afforded information on the morphology and composition of the gels formed. Here also, a clear distinction was observed between the gels precipitating in systems without additional silicon and the systems with that addition, whose Si/Al ratios were higher and similar to one another, confirming the ^{29}Si NMR and HCl attack findings. Zeolites were observed to form in all systems.

In light of the similarities between the AAFA WG and AAFA N10-15 systems revealed by the analysis of the mechanical properties, degree of reaction and microstructure of alkali-activated fly ash paste, waste glass may be regarded as an alternative to sodium silicates in the preparation of geopolymers.

Increasing efforts have been committed by leading practitioners from both academia and industry, to demonstrate the suitability of using AAMs in various concrete applications. Customers in different market areas are becoming more and more aware of technical progress in the development of non-Portland binders systems, and AAMs are a class of materials which are ideally positioned to take advantage of this awareness. Although there are still great challenges facing AAM producers, concerted commercialisation efforts in parallel with ground breaking research will be the only path forward to reach the final goal of large-scale deployment of this technology.

5. Acknowledgements

The present research was funded by the Spanish Ministry of Economy and Competitiveness under project BIA2010-15516. The authors wish to thank P. Rivilla for her invaluable assistance with the laboratory trials.

References

Alonso, S., Palomo, A., 2001. Calorimetric study of alkaline activation of calcium hydroxide-metakaolin solid mixtures. Cem. Concr. Res. 31, 25-30.

Bernal, S.A., Krivenko, P.F., Provis, J.L., Puertas, F., Rickard, W.D.A., Shi, C., Riessen, A., 2014.Other potential applications for alkali-activated materials. In: Provis J.L, van Deventer JSJ editors. Alkali-Activated Materials, State of the art report, RILEM TC 224-AAM. Springer, New York, London; pp. 339-379.

Breck, D.W., 1973. Zeolite molecular sieves: Structure, Chemistry and Uses, ed. Wiley, New York.

Brykov, A.S., Korneev, V.I., 2008. Production and usage of powdered alkali metal silicate hydrates. Metallurgist 52, 11-12.

Criado, M., Palomo, A., Fernández-Jiménez, A., 2005. Alkali activation of fly ashes. Part I: Effect of curing on the carbonation of the reaction products. Fuel 84, 2048-2054.

Criado, M., Fernández-Jiménez, A., de la Torre, AG., Aranda, M.A.G., Palomo, A., 2007. An XRD study of the effect of the SiO_2/Na_2O ratio on the alkali activation of fly ash. Cem. Concr. Res. 37, 671-679.

Criado, M., Fernández-Jiménez, A., Palomo, A., Sobrados, I., Sanz, J., 2008. Effect of the SiO_2/Na_2O ratio on the alkali activation of fly ash. Part II: ^{29}Si MAS-NMR Survey. Microporous Mesoporous Mater. 109, 525-534.

Davidovits, J., 1991. Geopolymers: inorganic polymeric new materials. J. Therm. Anal. 37, 1633-1656.

ECOBA., 2014. European Association for use of the By-products of Coal-Fired Power-Stations http://www.ecoba.com

El-Shamy, T.M., Lewis, J., Douglas, R.W., 1972. The dependence on the pH of the descomposition of glasses by aqueous solutions. Glass Technol. 13, 81-87.

El-Shamy, T.M., Panteno, C.G., 1977. Descomposition of silicates glasses in alkaline solutions. Nature 266, 704-706.

Engelhardt, G., Michel, D., 1987. High Resolution solid state NMR of silicates, Zeolite. ed. Wiley, London, England.

Fernández-Jiménez, A., Palomo, J.G., Puertas, F., 1999. Alkali-activated slag mortars: Mechanical strength behaviour. Cem. Concr. Res. 29(8), 1313-1321.

Fernández-Jiménez, A., Palomo, A., 2003a. Characterisation of fly ashes. Potential reactivity as alkaline cements. Fuel 82, 2259-2265.

Fernández-Jiménez, A., Palomo, A., 2003b. Alkali-activated fly ashes: properties and characteristics. 11th International Congress on the Chemistry of Cement, Durban, South Africa. 3, 1322-1340.

Fernández-Jiménez, A., Palomo, A., 2005a. Composition and microstructure of alkali activated fly ash binder: Effect of the activator. Cem. Concr. Res. 35, 1984-1992.

Fernández-Jiménez, A., Palomo, A., 2005b. Mid-Infrared Spectroscopy studies of alkali-activated fly ash structure. Microporus Mesoporus Mater. 86, 207-214.

Fernández-Jiménez, A., Palomo, A., López-Hombrados, C., 2006a. Engineering properties of alkali activated fly ash concrete. ACI Mater. J. 103(2), 106-112.

Fernández-Jiménez, A., de la Torre, A.G., Palomo, A., López-Olmo, G., Alonso, M.M., Aranda, M.A.G., 2006b. Quantitative determination of phases in the alkaline activation of fly ash. Part II: Degree of reaction. Fuel 85, 1960-1969.

Fernández-Jiménez, A., Palomo, A., Sobrados, I., Sanz, J., 2006c. The role played by the reactive alumina content in the alkaline activation of fly ashes. Microporus Mesoporus Mater. 91, 111-119.

Fernández-Jiménez, A., García-Lodeiro, I., Palomo, A., 2007. Durability of alkali-activated fly ash cementitious materials. J. Mater. Sci. 42, 3055-3065

Fernández Navarro, J.M., 2003. The Glass (El vidrio). Consejo Superior de Investigaciones Científicas. Sociedad Española de Cerámica y Vidrio, Madrid.

Glukhovsky, V.D., 1965. Their properties, technology and manufacturing and fields of application. PhD. Thesis, Civil Engineering Institute, Kiev, Ukraine.

Glukhovsky, V.D., 1989. In: Proceedings of the 2nd International Seminar on "Some Aspects of Admixtures and Industrial By-products on the Durability of Concrete". Gothenburg, Sweden, June 26-27, 53-62.

Gomes, S., François, M., 2000. Characterization of mullite in silicoaluminous fly ash by XRD, TEM, and ^{29}Si MAS NMR. Cem. Concr. Res. 30, 175-181.

Goto,K.J., 1955. States of silica in aqueous solution. II. Solubility of amorphous silica. J. Ceram. Soc. Jpn. 76, 1364-1366.

Hardjito, D., Wallah, S.E., Rangan, BV., 2002. Research into Engineering Properties of Geopolymer Concrete. International Conference "Geopolymer 2002 – tur potential into profit", Melbourne, Australia.

Hendriks, C.A., Worrell, E., deJager, D., Block, K., Riemer, P., 2000. Emission reduction of greenhouse gases from the cement industry, IEA Greenhouse gas R&D Programme. Available from: http://www.ieagreen.org.uk/prghgt42.htm

Huntizinger, D.N., Eatmon, T.D., 2009. A life-cycle assessment of Portland cement manufacturing: comparing the traditional process with alternative technologies. J. Clean. Prod. 17, 668-675.

Klinowski, J., 1984. Nuclear magnetic resonance studies of zeolites. Pro. Nucl. Magn. Reson. Spectrosc. 16, 237-309.

Kovalchuk, G., 2002. Heat resistant gas concrete based on alkaline aluminosilicate binder. PhD Thesis, Kyiv, Ukrainian.

Kovalchuk, G., Fernández-Jiménez, A., Palomo, A., 2007. Alkali-activated fly ash: Effect of termal curing conditions on mechanical and microstructural development-Part II" Fuel 86, 315-322.

Krivenko, P.V., 1994. Alkaline cements. First Int. Conf. on Alkaline Cements and Concrete, Kiev, Ukraine. 1, 11-129.

Krivenko, P.V., Kovalchuk, G., Yu., 2002a. Fly ash based Zeolite Cements. Innovations and developments in Concrete Materials and Construction: Proceed. Intern. Conf. "Challenges of Concrete Construction", Dundee, 123-132.

Krivenko, P.V., Kovalchuk, G., Yu., 2002b. Heat-resistant Fly Ash based geocements. Proceed. Intern. Conf. Geopolymers 2002, Melbourne.

Larosa-Thomson, J., Gill, P., Scheetz, B.E., Silsbee, M.R., 1997. Sodium silicate applications for cement and concrete. Proc. 10th Int. Congr. On the Chemistry of Cement, Gothenburg.Vol.3.3.

McCormick, A.V., Bell, AT., Radke, C.J., 1987a. Quantitative determination of siliceous species in sodium silicate solutions by ^{29}Si N.M.R Spectrosc. Zeolites. 7, 183-190.

McCormick, A.V., Bell, A.T., Radke, C.J., 1987b. Multinuclear NMR Investigation of the Formation of Aluminosilicate Anions. J. Phys. Chem. 93, 1741-1744.

Mejía, J.M., Mejía de Gutiérrez, R., Puertas, F., 2013. Rice husk ash as silica source in fly ash and ground blast furnace slag cementitious alkali activated systems. Mater. Construcc. 63 (311), 361-375.

Mendes, A., Sanjayan, J., Collins, F., 2008. Phase transformations and mechanical strength of OPC/slag pastes submitted to high temperatures. Mater. Struct. 41(2), 345-350.

Mendes, A., Sanjayan, J., Collins, F., 2009. Long-term progressive deterioration following fire exposure of OPC versus slag blended cement pastes. Mater. Struct. 42 (1), 95-101.

Mozgawa, W., Sitarz, M., Rokita, M., 1999. Spectroscopic studies of different aluminosilicate structures. J. Mol. Struct. 511-512, 251-257.

Palacios, M., Puertas, F., 2007. Effect of shrinkage-reducing admixtures on the properties of alkali-activated slag mortars and pastes. Cem. Concr. Res. 37(5), 691-702.

Palomo, A., Grutzeck, M.W., Blanco, M.T., 1999. Alkali activated fly ashes: a cement for the future. Cem. Concr. Res. 29(8), 1323-1329.

Palomo, A., López de la Fuente, J.L., 2003. Alkali-activated cementitous materials: Alternative matrices for the immobilisation of hazardous wastes: Part I. Stabilisation of boron. Cem. Concr. Res. 33, 281-288.

Palomo, A., Alonso, S., Fernández-Jiménez, A., Sobrados, I., Sanz, J., 2004a. Alkaline Activation of fly ashes: NMR study of the reaction products. J. Am. Ceram. Soc. 87(6), 1141-1145.

Palomo, A., Fernández-Jiménez, A., Criado, M., 2004b. Geopolymers: same basic chemistry, different microstructures (Geopolimeros: una única base química y diferentes microestructuras). Mater . Construcc. 54 (275), 77-91.

Paul, A., 1977. Chemical durability of glasses; a thermodynamic approach. J. Mater. Sci. 12, 2246-2268.

Provis, J.L., 2009. Activating solution chemistry for geopolymers. In: Provis J.L, van Deventer JSJ editors. Geopolymers: structures, processing, properties and Industrial Applications, Woodhead, Cambrige, UK;pp. 50-71.

Puertas, F., 1995. Alkali activated slag cements: current situation and future prospects (Cementos de escorias activadas alcalinamente: Situación actual y perspectiva de futuro). Mater. Construcc. 45 (239), 53-64.

Puertas, F., Torres-Carrasco, M., Varga, C., Torres, J.J., Moreno, E., Palomo, J.G., 2012a. Re-use of urban and industrial glass waste to prepare alkaline cements. 4th International Conference on Engineering for Waste and Biomass Valorisation, Oporto (Portugal).

Puertas, F., Torres, J.J., Varga, C., Torres-Carrasco, M., 2012b. Spanishpatent "Procedimiento para la fabricación de cementos alcalinos a partir de residuos vítreos urbanos e industriales" (Process for the manufacture of alkaline cements from urban and industrial wastes glasses). PCT/ES2012/070408.

Puertas, F., Torres-Carrasco, M., 2014. Use of glass waste as an activator in the preparation of alkali-activated slag cements. Mechanical strength and paste characterization. Cem. Concr. Res. 57, 95-104.

Rahier, H., Van Mele, B., Biesemans, M., Wastiels, J., Wu, X., 1996. Low-temperature synthesized aluminosilicate glasses. J. Mater. Sci. 31, 71-79.

Scrivener, K.L., Kirkpatrick R.L., 2007. Innovation in use and research on cementitious material. 12th International Congress of Chemistry of Cement, Montreal, (Canada).

Torres-Carrasco, M., Puertas, F., Blanco-Varela, M.T., 2012. Preparation of alkaline cements from waste glass. Solubility of waste glass in basic media (Preparación de cementos alcalinos a partir de residuos vítreos. Solubilidad de residuos vítreos en medios fuertemente básicos). XII Congreso Nacional de Materiales (Alicante).

Torres-Carrasco, M., Palomo, J.G., Puertas, F., 2014. Sodium silicate solutions form dissolution of glass wastes: Statistical analysis. Mater.Construcc.64 (314).

Ukqaa., 2014. http://www.ukqaa.org.uk

U.S. Environmental Protection Agency., 2004. Inventory of U.S. Greenhouse gas emissions and sinks.EPA 430-R-04-003.

Van Wazer, J.R., 1970. Equilibria and kinetics in inorganic polymerizations. Inorg. Macromol. 1, 89-99.

Weng, L., Sagoe-Crentsil, K., Brown, T., Song, S., 2005. Effects of aluminates on the formation of geopolymers. Mater. Sci. Eng., B. 117(2), 163-168.

Yang, K.H., Song, J.K., Song, K.I., 2013.Assessment of CO_2 reduction of alkali-activated concrete. J. Clean. Prod. 39, 265-272.

Yang, K.H., Jung, Y.B., Cho, M.S., Tae, S.H., 2014.Effect of supplementary cementitious materials on reduction of CO_2 emissions from concrete. J. Clean. Prod. In press. 10.1016/j.jclepro.2014.03.018

Zeng, Q., Li, K., Fen-chong, T., Dangla, P., 2010. Pore structure characterization of cement pastes blended with high-volume fly-ash. Cem. Concr. Res. 42, 194-204.

Tables and Figures

List of Tables:

List of Figures:

Table 1. Chemical composition of fly ash and waste glass (wt.%)

(wt.%)	CaO	SiO_2	Al_2O_3	MgO	Fe_2O_3	Na_2O	K_2O	TiO_2	[1]L.O.I
Fly Ash	2.72	54.44	27.51	1.51	6.38	1.51	3.13	1.27	2.1
Glass waste	11.75	70.71	2.05	1.17	0.52	11.71	1.08	-	0.83

[1]L.O.I = Loss on ignition

Table 2. Reactive SiO_2 and Al_2O_3 content in fly ash

	Vitreous phase[a](%)	ReactiveSiO_2[b] (%)	Reactive Al_2O_3[a](%)	Reactive SiO_2[b] + Al_2O_3[a] (%)	Si/Al (atomic ratio)	SiO_2/Al_2O_3
Fly ash	61.08	45.05	18.04	63.09	1.42	1.97

[a]Determined by acid attack with 1-% HF

[b] Determined as stipulated in Spanish standard UNE 80-225-93

Table 3. SiO_2, Al_2O_3, CaO and MgO content (g/100 ml) in solutions prepared by dissolving waste glass in 100 mL of 10-M NaOH

Amount of glass waste	SiO_2 (g/ 100 ml)	Al_2O_3 (g/ 100 ml)	CaO (g/ 100 ml)	MgO (g/ 100 ml)	pH
10 g	3.078	0.095	2.73 E-4	2.82 E^{-4}	13.6
15 g	3.638	0.117	3.12 E-4	4.12 E^{-4}	13.4
25 g	4.94	0.182	4.24 E-4	1.94 E^{-3}	12.9

Table 4. Geopolymer preparation: activation conditions

Sample name	Activator type	L/S	Glass waste content	(%) Na_2O	(%) SiO_2	SiO_2/Na_2O	ρ (g/cm^3)	pH
***AAFA N8**	NaOH 8M	0.3	-	5.27	-	0	1.27	13.9
***AAFA N10**	NaOH 10M	0.3	-	6.43	-	0	1.30	14.1
***AAFA WG**	NaOH 10M + 15% WG	0.3	-	5.60	1.09	0.19	1.35	13.8
***AAFA N10-10g**	NaOH 10 M	0.3	10 g	6.43	0.64	0.10	1.30	13.6
***AAFA N10-15g**	NaOH 10 M	0.3	15 g	6.43	0.75	0.11	1.30	13.4
***AAFAN10-25g**	NaOH 10 M	0.3	25 g	6.43	1.03	0.16	1.30	12.9

AAFA N8 = alkali activated fly ash with NaOH 8M

AAFA N10 = alkali activated fly ash with NaOH 10M

AAFA WG = alkali activated fly ash with NaOH10M + 15% WG

AAFA N10 -10g,15g,25g = alkali activated fly ash with NaOH 10M and from 10 to 25 g of waste glass

Table 5.Deconvolution of the ^{29}Si MAS NMR spectrum for fly ash

Sample										
Anhydrous FA	δ (ppm)	-78.59	-83.77	-89.21	-94.82	-99.72	-104.38	-108.9	-113.39	-118.67
	Width	5.20	5.20	5.20	5.20	5.20	5.20	5.20	5.20	5.20
	Integral (%)	1.25	2.66	8.37	12.18	18.36	19.12	17.51	13.51	7.03

Table 6.^{29}Si NMR signals for 7-day alkali activated fly ash

Sample		Residual xylanol group	Aluminosilicate gel					Q_x^{4b}	Ref. zeolite[c]	$(Si/Al)^d_{NMR}$
			Si(4Al)	Si(4Al)	Si(3Al)	Si(2Al)	Si(1Al)	Si(0Al)		
AAFA N8	δ (ppm)	-	-83.14	-88.1	-93.12	-98.81[a]	-104.86	-110.29	-115.98		
	Width	-	5.20	5.20	5.20	5.20	5.20	5.02	5.20	H, C	1.85
	Integral (%)	-	5.85	13.42	15.58	23.67	21.01	13.5	6.98		
AAFA WG	δ (ppm)	-	-84.3	-88.77	-93.52	-98.75[a]	-103.9	-108.29	-113.06		
	Width	-	5.20	5.20	5.20	5.20	5.20	5.20	5.20	H, C	2.04
	Integral (%)	-	8.71	11.1	16.62	25.69	16.95	12.72	8.21		
AAFA N10-15	δ (ppm)	-77.95	-83.99	-87.88	-93.15	-98.80	-104.72	-110.21	-115.08		
	Width	5.20	5.20	5.20	5.20	5.20	5.20	5.20	5.20	H, C	2.01
	Integral (%)	1.92	4.49	12.42	17.73	25.70	21.00	11.59	5.16		

[a] Highest intensity peak
[b]Silica polymorphs : quartz (-108 ppm); coesite (-108, -113.9 ppm); cristobalite (-108.5); tridymite (-109 to -114 ppm)
[c] H = hydroxysodalite; C = chabazite-Na
[d] Calculated from the Engelhard equation

Table 7. Degrees of reaction, percentage of dissolved silica and alumina after a selective 1:20 HCl attack on alkali-activated systems. SiO_2/Al_2O_3 ratio of the reaction products

Degree of reaction		Composition of reaction products (wt.%)			
Sample	**(%)**	**SiO_2**	**Al_2O_3**	**$SiO_2 + Al_2O_3$**	**SiO_2/Al_2O_3**
AAFA N8	28.80	26.60	15.10	41.70	1.76
AAFA WG	31.60	42.77	20.53	63.30	2.08
AAFA N10-15	34.10	29.00	15.28	44.28	1.89

Table 8. BSEM/EDX-determined chemical composition of 7-day sodium aluminosilicate gel obtained by activating fly ash with three solutions

Activating solution	Si	Al	Na	Si/Al	Na/Al
AAFA N8	18.74 ± 1.40	10.64 ± 2.40	5.90 ± 1.97	1.86 ± 0.50	0.61 ± 0.32
AAFA WG	19.79 ± 0.92	9.62 ± 1.08	7.30 ± 2.30	2.08 ± 0.22	0.78 ± 0.30
AAFA N10-15	19.61 ± 0.50	9.53 ± 0.96	7.79 ± 1.85	2.08 ±0.20	0.84 ± 0.27

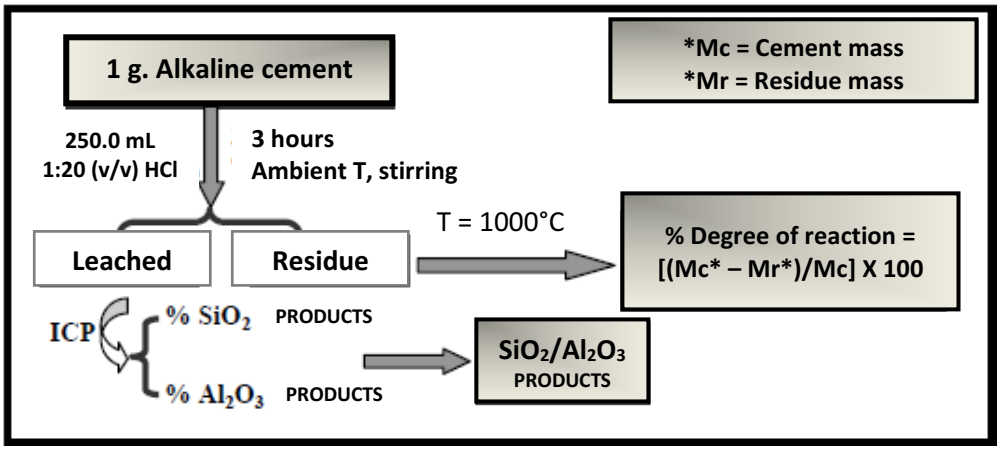

Figure 1. Experimental method for quantifying the degree of reaction of the alkali cements prepared and the SiO_2/Al_2O_3 ratios of the reaction products generated during alkali activation

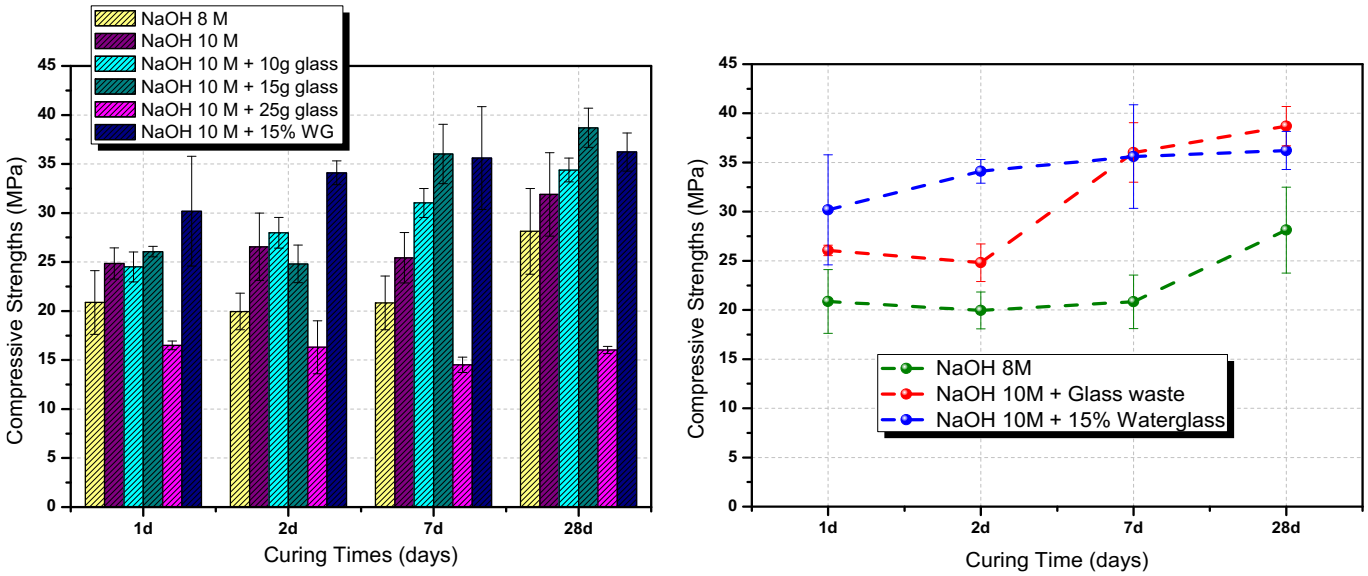

Figure 2. a) Compressive strength of fly ash pastes activated with different alkaline solutions; b) compressive strength of specimens prepared withNaOH 8M, NaOH 10M + 15 % WG and NaOH 10M + 10, 15 or 25 g of waste glass

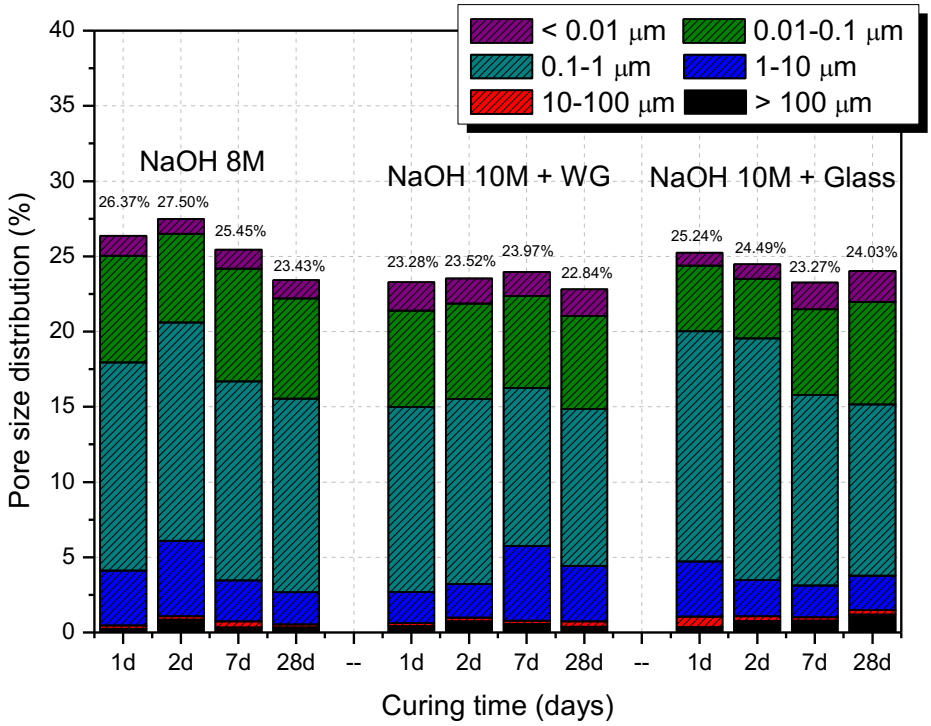

Figure 3. Pore size distribution inNaOH 8M, NaOH 10M + WG and NaOH 10M + glass AAFA

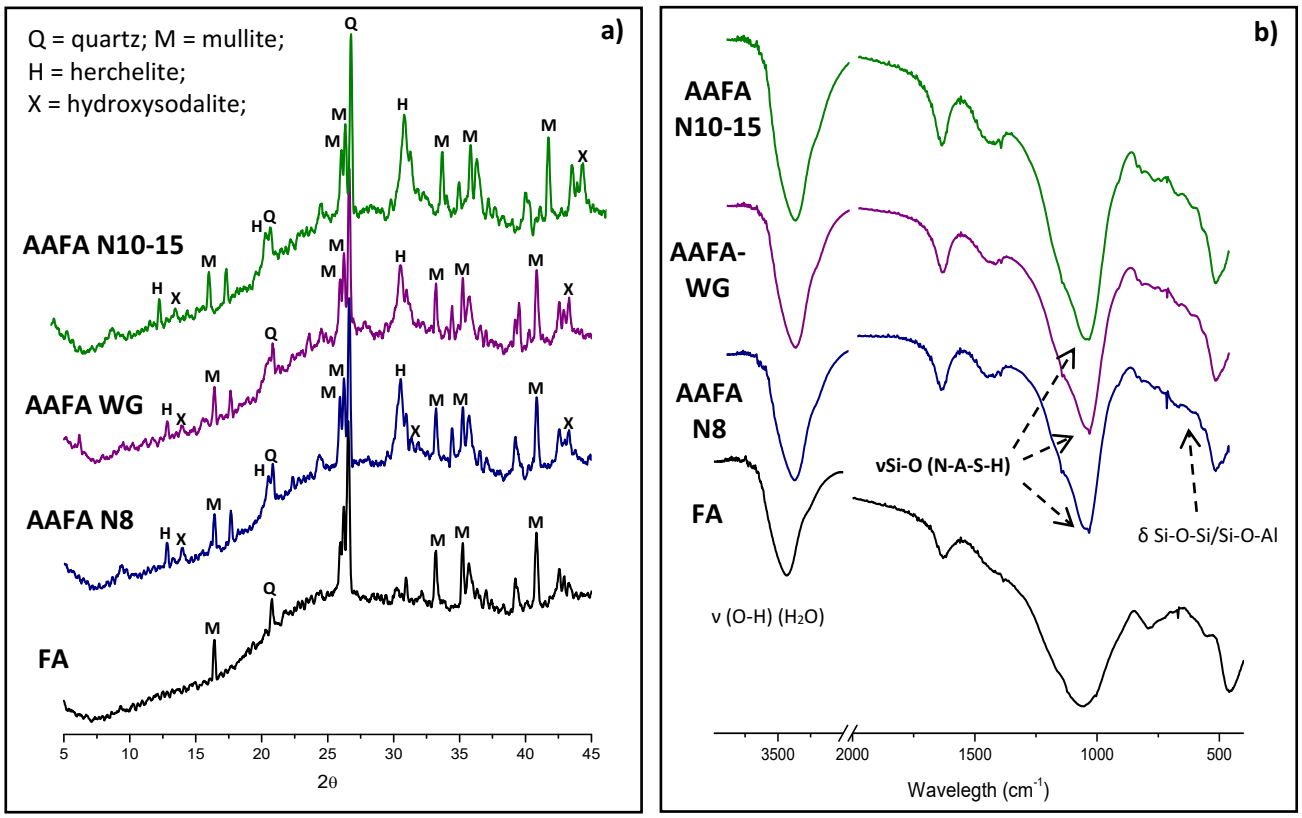

Figure 4. a) XRD for fly ash and alkali-activated fly ash pastes; b) FTIR spectra for fly ash and alkali-activated fly ash pastes.

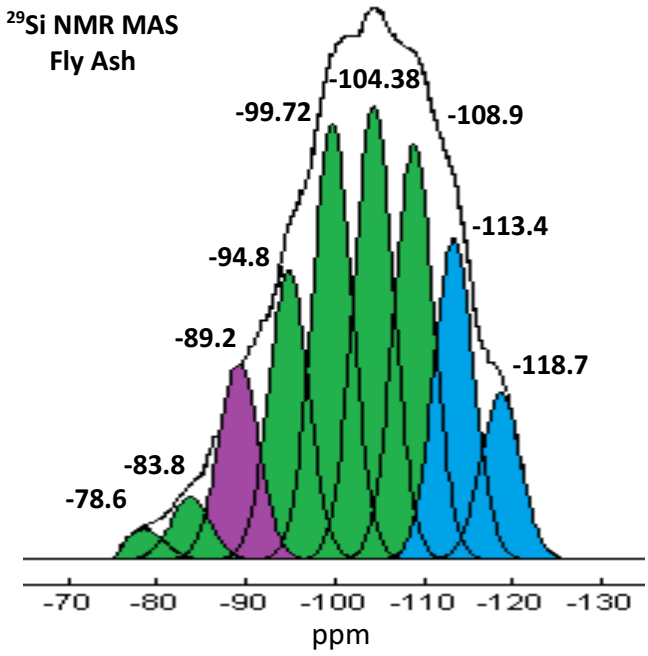

Figure 5.[29]Si NMR spectra for the starting fly ash

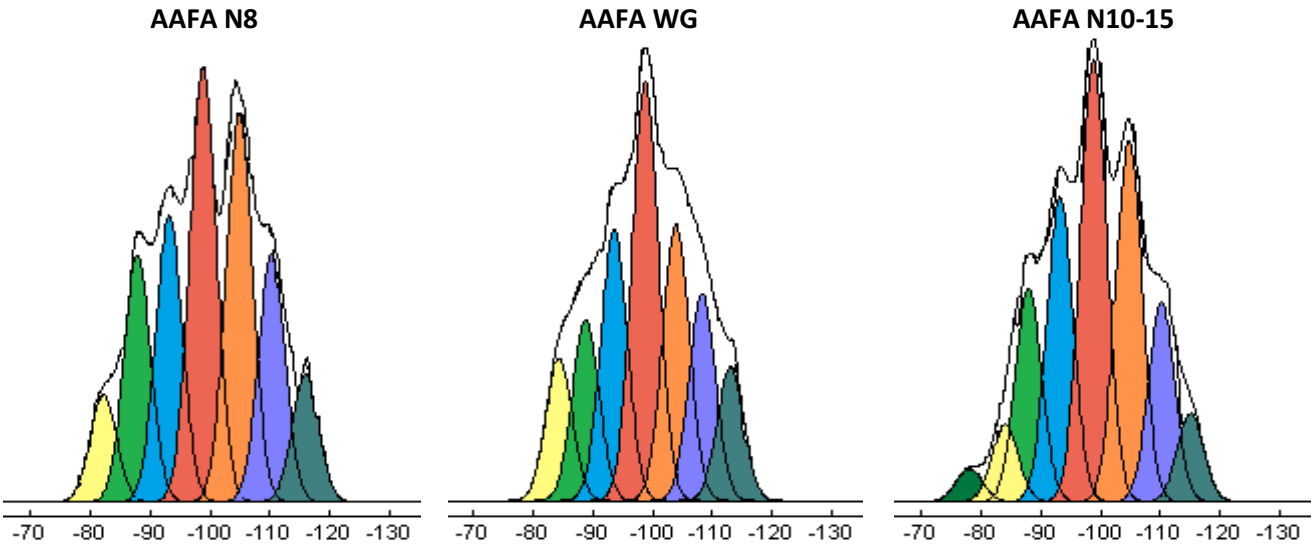

Figure 6.[29]Si MAS NMR spectra of alkali activated fly ash pastes: AAFA N8, AAFA WG and AAFA N10-15.

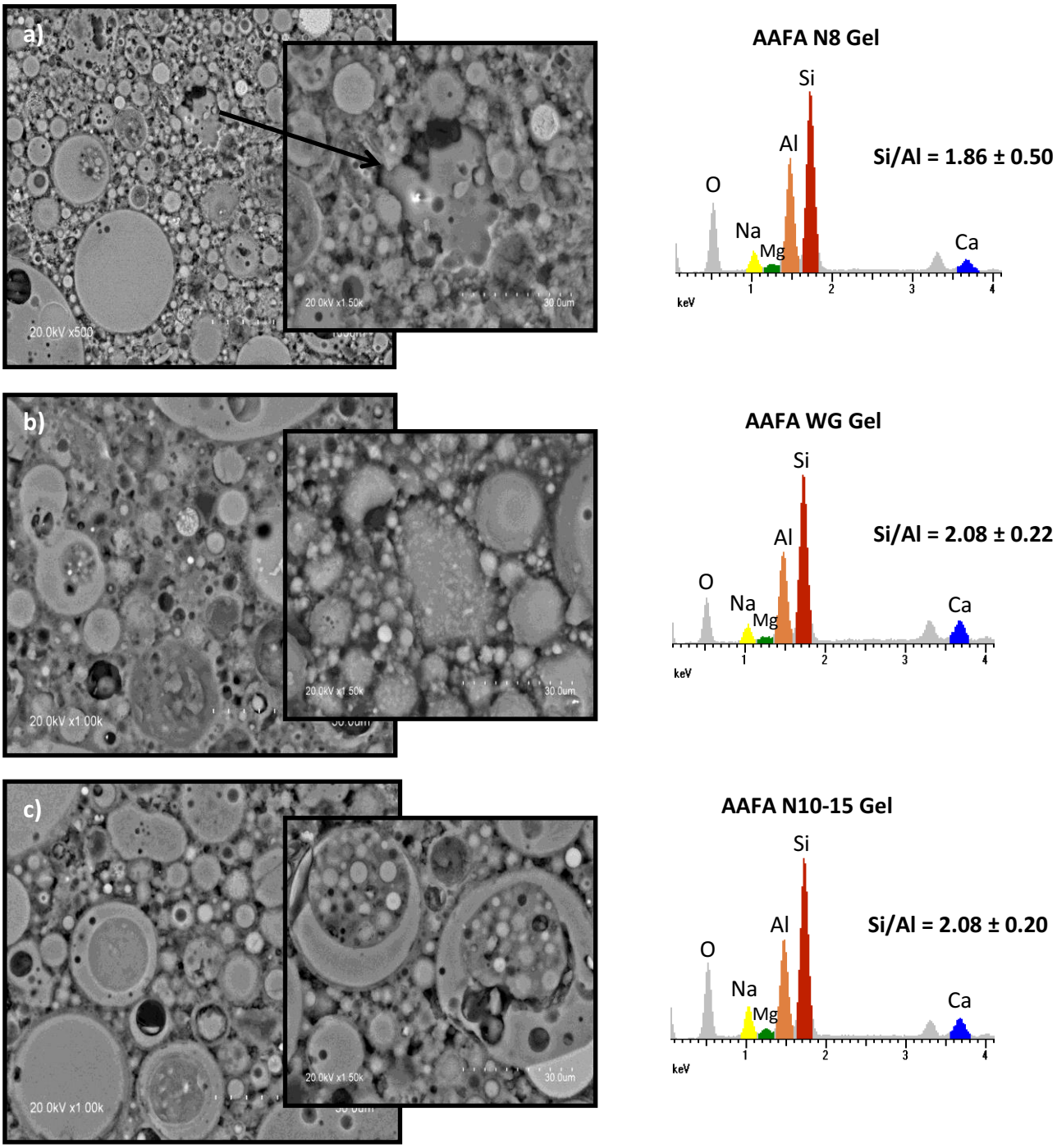

Figure 7. BSEM/EDX images of a) AAFA N8, b) AAFA WG, c) AAFA N10-15 pastes

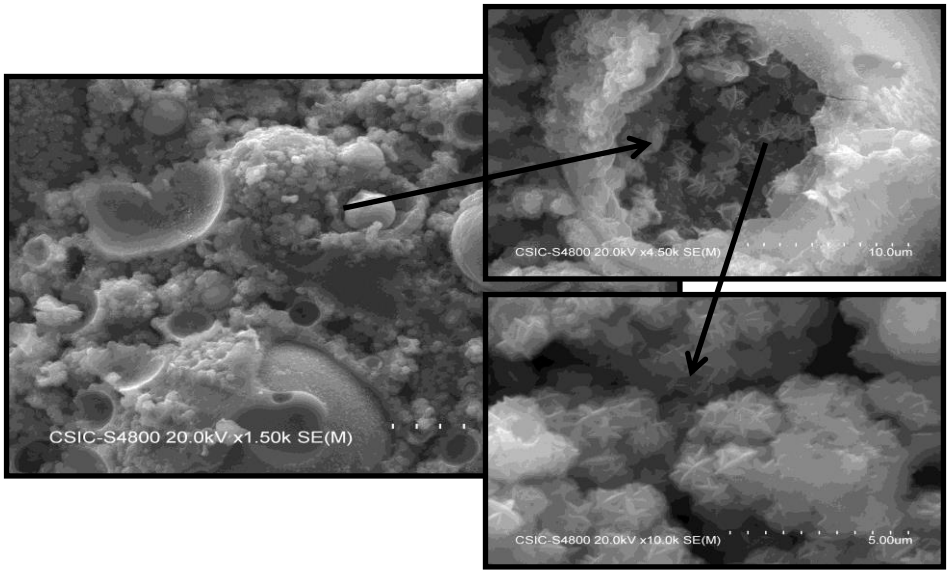

Figure 8. Detail of crystalline phases (chabazite-Na-like zeolite) formed in fly ash pastes activated with NaOH 8M (**AAFA N8**)

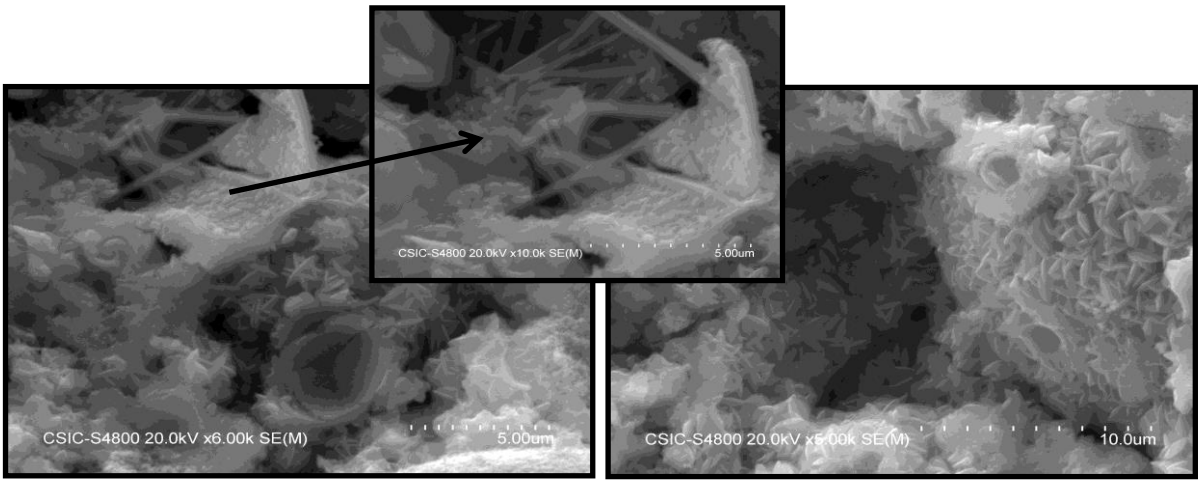

Figure 9. Detail of crystalline phases (chabazite-Na-like zeolite) formed in fly ash pastes activated with NaOH 10M+ 15 % WG (**AAFA WG**)

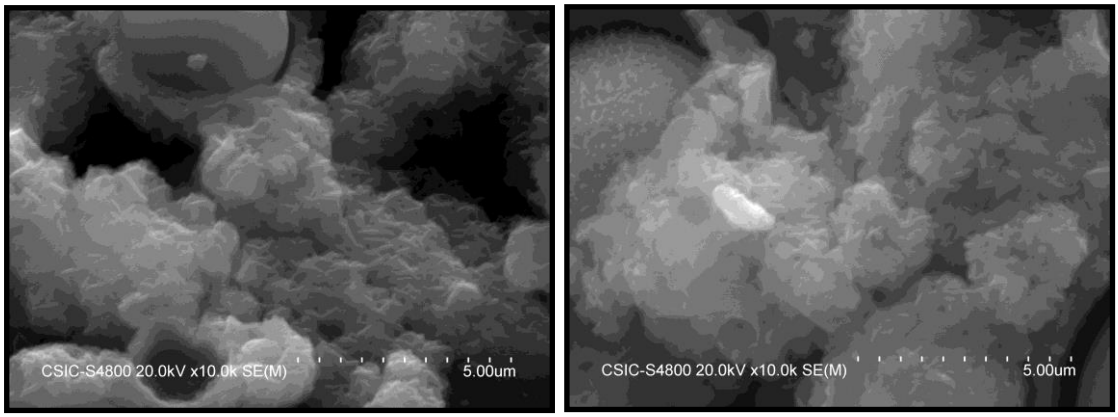

Figure 10. Detail of crystalline phases (chabazite-Na-like zeolite) formed in fly ash pastes activated with NaOH 10M + glass (**AAFA N10-15**)